

Pressure-induced order-disorder transitions in RNi_2 compounds

A. Lindbaum and E. Gratz

Vienna University of Technology, Institute for Experimental Physics, Wiedner Hauptstrasse 8-10/131, A-1040 Wien, Austria

S. Heathman

Joint Research Center, European Commission, Institute for Transuranium Elements, Postfach 2340, D-76125 Karlsruhe, Germany

(Received 31 May 2001; revised manuscript received 8 November 2001; published 26 March 2002)

Most of the RNi_2 compounds (R =rare-earth element) do not crystallize in the cubic Laves phase structure ($C15$), but in a superstructure of $C15$ with ordered vacancies at the R sites. In the present work high pressure x-ray diffraction experiments on selected RNi_2 compounds (R =Tb,Sm,Gd, and Y) are presented, showing that pressures of about 8–15 GPa lead to a disordering of the vacancies in all of them. Furthermore the studies show that the pressure-induced order-disorder transition is closely related to the earlier observed disordering of the vacancies at high temperatures between 430 (TbNi₂) and 740 K (YNi₂), and that there is a pronounced variation of the transition pressures and temperatures among the investigated compounds. The driving mechanism behind these transitions is discussed.

DOI: 10.1103/PhysRevB.65.134114

PACS number(s): 61.10.Nz, 61.50.Ks, 61.66.-f, 61.66.Fn

I. INTRODUCTION

The RNi_2 compounds (R =rare-earth element) are often considered to show the cubic Laves phase structure ($C15$), but recent experimental as well as theoretical investigations showed that this is not true. Instead of showing the pure $C15$ structure, most of them crystallize in a superstructure of $C15$ with ordered vacancies at the R sites and with doubled lattice parameter. The first detailed analysis of this $C15$ superstructure was performed for YNi₂, showing that a single phase compound can only be obtained with the stoichiometry 0.95:2 and can be described within space group $F\bar{4}3m$ with the $4a$ sites only partially occupied by the Y atoms.¹ A systematic investigation of the $R_{1-x}Ni_2$ compounds revealed that this superstructure exists also for other R elements, however, the occupancy of the R $4a$ sites increases with decreasing radius of the R atom and reaches 1 for LuNi₂.² For simplicity, the notation RNi_2 will be used throughout the paper (instead of the correct notation $R_{1-x}Ni_2$).

When proceeding from the RNi_2 to the RCu_2 compounds, the crystal structure changes completely. The RCu_2 compounds with R from Ce to Lu show the orthorhombic CeCu₂ type of structure, a distorted variant of the hexagonal AIB₂ type (which is the crystal structure of LaCu₂). In contrast to the $C15$ structure the R and Cu atoms are separately stacked forming a layered structure. According to *ab initio* total energy calculations this structural change is caused by electronic band structure effects.³ On the other hand, the instability of the $C15$ structure in the RNi_2 compounds (i.e., the tendency towards the formation of vacancies) can be understood by space filling arguments. Recent theoretical investigations, also based on *ab initio* total energy calculations, showed that the vacancies at the R sites lower the total energy, thus increasing the stability relative to the neighboring compounds in the R -Ni phase diagram.⁴ The existence of the vacancies allow for a relaxation of the lattice, leading to an increase of all R - R distances and releasing internal strains on the R sublattice.

The existence of ordered R vacancies in the RNi_2 compounds is not only important for understanding the mechanisms stabilizing the crystal structure, but must also be taken into account when investigating other physical properties, such as, e.g., the magnetic structure. The ordered vacancies change the local surrounding of the R sites, leading to a change of the crystal field as well as the magnetic exchange interactions. As an example, recent investigations on TbNi₂ showed that the ordered vacancies at the Tb sites are responsible for a temperature induced change of the magnetic structure at 14 K.⁵

An interesting property of the RNi_2 superstructures is a reversible temperature induced transition from ordered to disordered vacancies at high temperatures, first detected by anomalies in the transport properties and later directly observed by x-ray diffraction experiments.⁶ Preliminary results from high-pressure x-ray diffraction experiments on YNi₂, reported in the same paper,⁶ showed that there is also a pressure-induced order-disorder transition.

The subject of the present work is a detailed high-pressure x-ray diffraction study of the pressure-induced structural transition in the RNi_2 superstructures, and a discussion of the driving mechanism. For this purpose the four compounds TbNi₂, GdNi₂, SmNi₂, and YNi₂, which have already been studied with respect to the temperature-induced transition,⁶ have been selected.

II. EXPERIMENT

A. Sample preparation

Polycrystalline samples of TbNi₂, GdNi₂, SmNi₂, and YNi₂ were prepared by induction melting in a water cooled copper crucible. For obtaining single phase samples of the $C15$ superstructure with ordered R vacancies it was necessary to take a stoichiometry deviating from 1:2 (0.95:2 for GdNi₂, SmNi₂, YNi₂, and 0.96:2 for TbNi₂), and to anneal the samples after melting for one month at 650 °C. The phase purity was checked by x-ray diffraction and electron

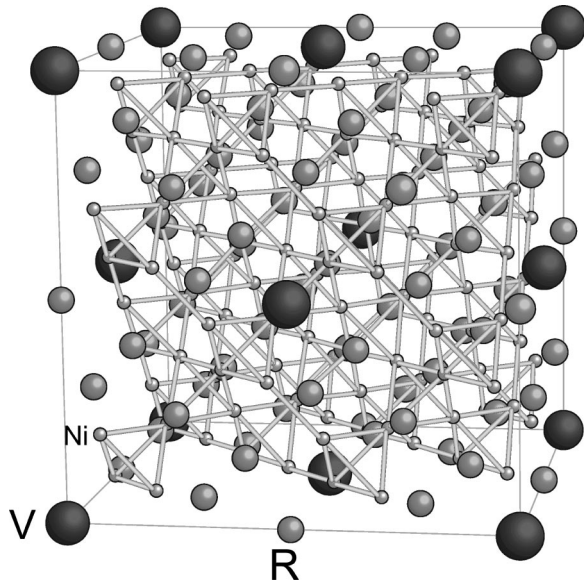


FIG. 1. The cubic superstructure cell of the investigated RNi_2 compounds. The $4a$ positions of the R atoms (where the ordered vacancies are located) are marked by the big black spheres (V). The tetrahedral Ni framework is indicated by the bonds.

microprobe analysis. With the 1:2 stoichiometry one obtains the superstructure as main phase and the R -richer 1:1 phase as impurity, i.e., it is not possible to obtain the pure $C15$ structure without ordered vacancies for these RNi_2 compounds.

B. High-pressure x-ray diffraction experiments

The high-pressure x-ray diffraction experiments (HPXRD) were performed at the ELETTRA (Trieste, Italy) synchrotron radiation facility in the angle dispersive mode using a two-dimensional (2D) image plate detector (x-ray diffraction beamline), and at the storage ring DORIS III of HASYLAB (DESY synchrotron, Hamburg, Germany) in the energy dispersive mode using a Germanium detector (F3 beamline). The x-ray wavelength used in the angle dispersive experiments at ELETTRA was 0.69 Å.

The powdered samples were loaded into a 0.25 mm hole drilled into an annealed (800 °C for three hours) and preindented Inconel gasket together with a small ruby crystal (for pressure determination via the ruby fluorescence method) or quartz powder (for pressure determination via the known pressure dependence of the lattice parameters of quartz⁷). The diameter of the flat parts of the diamonds (which generate the pressure) was 0.6 mm. As pressure transmitting medium a 4:1 methanol-ethanol mixture was used. The used diamond anvil cell was a Syassen-Holzapfel⁸ cell, which is well suited for small pressure steps.

III. CRYSTAL STRUCTURES

At ambient conditions the structure of the investigated RNi_2 compounds is a superstructure of $C15$ and can be described within the space group $F\bar{4}3m$, with doubled lattice parameter a compared to the $C15$ structure (see Fig. 1). The

R atoms are located at five different crystallographic sites, whereas the ordered vacancies are only located at one of these 5 sites, namely, the $4a$ sites.¹ However, the $4a$ sites are not completely empty, and the occupancy varies among the investigated RNi_2 compounds. This variation is due to the different sizes of the different R atoms,² but, as explained in the next paragraph, the occupancy can also depend on other factors, such as, e.g., the starting stoichiometry of the samples.

The existence of a homogeneity range for the occupancy of the $4a$ sites can be demonstrated by a comparison of two different $TbNi_2$ samples: The $TbNi_2$ sample, used in the present work, had a starting stoichiometry of 0.96:2 and Rietveld refinements gave an occupancy value for the $4a$ sites of about 0.75. This value corresponds to a composition of 0.984:2 and is in good agreement with the value of 0.98:2, which has been determined by electron microprobe analysis for the same sample.⁵ However, as reported earlier, it is also possible to obtain a single phase sample with a $4a$ occupancy of only 0.29, which corresponds to a composition of 0.956:2.² This means that there is obviously a relatively large range of homogeneity for the numbers of the ordered vacancies (but note, that it is not possible to obtain samples without ordered vacancies). The YNi_2 sample, used in the present work, was prepared with a starting stoichiometry of 0.95:2, and Rietveld refinements¹ as well as x-ray studies on a single crystal⁶ gave a $4a$ occupancy of 0.25 and 0.24, respectively, both corresponding to a composition of 0.953:2. Identifying all the details in the sample preparation procedure, which can have an influence on the occupancy of the $4a$ sites, is still an open question, and should be a topic of further investigations.

IV. RESULTS

A. $TbNi_2$

Among the four studied RNi_2 compounds, $TbNi_2$ was investigated in most details. The reason for this was twofold: first, as already mentioned in the introduction, this compound is very interesting with regard to a change of the magnetic structure at 14 K, which is caused by the existence of the ordered vacancies at the Tb sites, and second, the transition temperature of the temperature-induced order-disorder transition is lowest in this compound (about 430 K).⁶

The HPXRD experiments on $TbNi_2$ clearly show the existence of a pressure-induced structural transition from the $C15$ superstructure to a structure with $C15$ symmetry. The transition can easily be detected by the disappearance of the additional x-ray lines which are caused by the lower translational symmetry in the superstructure. For illustrating the disappearance of these superstructure lines, Fig. 2 shows the 2D x-ray diffraction images of $TbNi_2$ at 0 and 14.8 GPa, obtained by angle dispersive experiments using a 2D image plate detector.

For determining the diffraction angles and intensities of the x-ray lines as a function of pressure we integrated over the diffraction rings of all the obtained 2D images using the FIT2D program.⁹ It is possible to estimate the transition pressure by following the pressure-induced variation of the in-

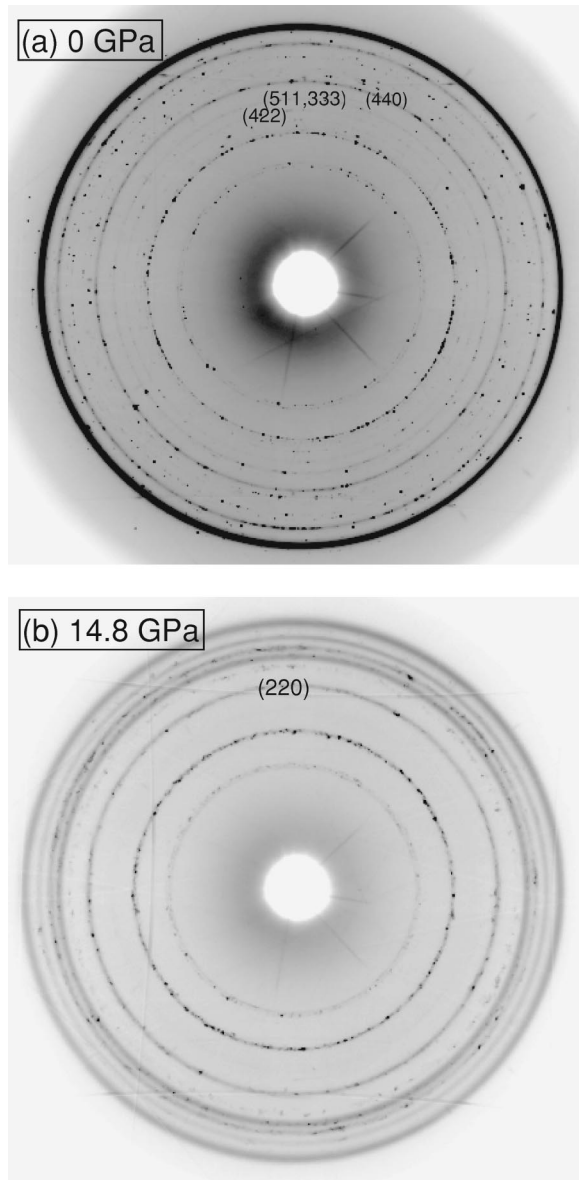


FIG. 2. The figure shows the 2D images of the x-ray diffraction rings of TbNi₂ and quartz (pressure calibrant) at 0 (a) and 14.8 GPa (b), respectively. At 14.8 GPa the additional diffraction lines caused by the lower translational symmetry of the C15 superstructure are no longer visible. For illustrating this, the two strongest of these additional lines (511,333) and (422), as well as the (220) line of the C15 structure [(440) in the superstructure description] are marked. The strong diffraction ring near the edge of the images is the first line of the gasket material, which was hit by the incident x-ray beam.

tensity of the strongest superstructure line (511,333) relative to the intensity of the (440) line [which corresponds to (220) of the C15 symmetry]. The result of this analysis is shown in Fig. 3 and leads to an estimated transition pressure of 8 ± 2 GPa. This estimation is not very precise, since the disappearance of the superstructure line is more or less continuous between 6 and 15 GPa, very similar to the temperature-induced disappearance of the superstructure line observed by high-temperature x-ray diffraction.⁶ (We defined the transi-

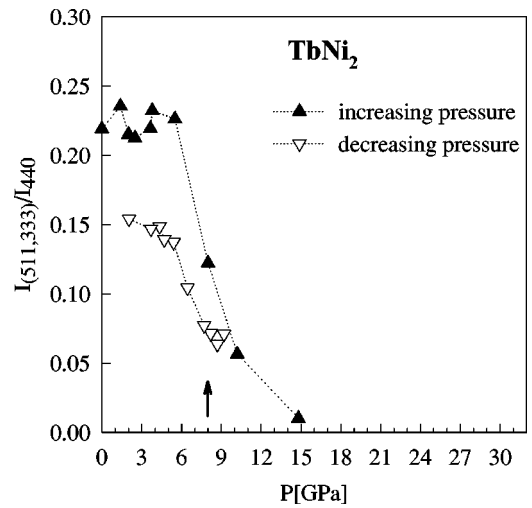


FIG. 3. Intensity ratio of the strongest superstructure line (511,333) and the (440) line [corresponding to (220) of C15] as a function of pressure for TbNi₂, illustrating the pressure-induced transition from the C15 superstructure to a structure with C15 symmetry at about 8 GPa (arrow).

tion pressure as the pressure where the intensity of the superstructure line has decreased to about 50%. This enables a quantitative comparison concerning the stability of the superstructure against pressure in the different investigated samples, which, with the exception of YNi₂, all show more or less smeared transitions.) When releasing the pressure (open symbols in Fig. 3) the superstructure lines appear again, indicating the reversibility of the transition. However, the reverse transition is not complete, which can be seen by the lower intensity of the (511,333) superstructure line after pressure release. This may be due to internal strains, which remain after pressure release and inhibit a complete retransformation.

Figure 4 shows the variation of the volume of TbNi₂ as a function of the applied pressure. The solid line is the result of fitting the Murnaghan equation of state (EOS) function to the experimental data.¹⁰ There is no anomaly in the *P*-*V* curve and the obtained values for the bulk modulus $K_0=103 \pm 3$ GPa and $K'_0=5.9 \pm 0.2$ indicate a normal compressibility, which is typical for intermetallic compounds.¹¹ The error bars have been estimated by carrying out the EOS fit proce-

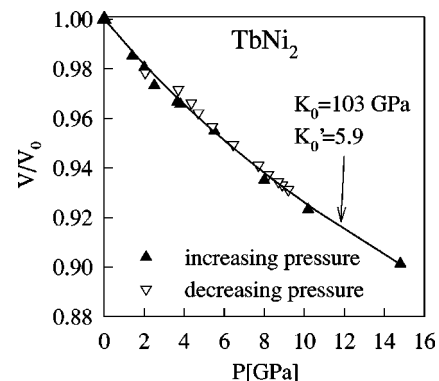


FIG. 4. Relative volume as a function of pressure for TbNi₂.

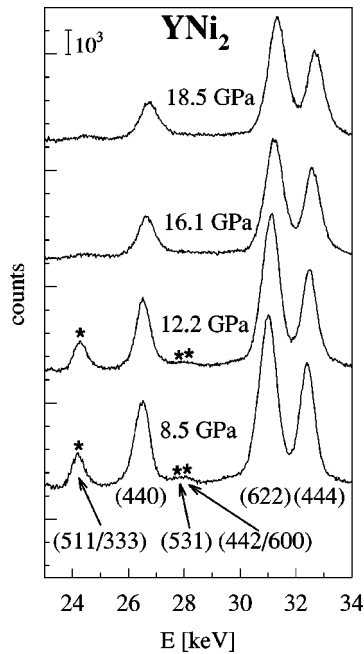


FIG. 5. Energy dispersive x-ray patterns of YNi_2 for four pressures around the pressure-induced transition. The asterisks indicate additional reflections, which are only present in the superstructure.

ture for various pressure ranges and using also other EOS models, such as, e.g., the Birch model.¹²

B. YNi_2 , SmNi_2 , and GdNi_2

The results of HPXRD experiments on the other three investigated $R\text{Ni}_2$ compounds, which were performed using the energy dispersive technique, show, as for TbNi_2 , a pressure-induced structural transition from the $C15$ superstructure to a structure with $C15$ symmetry. For illustrating the evolution of the energy dispersive x-ray patterns through the observed phase transition, Fig. 5 shows as an example some measured patterns of YNi_2 around the transition.

Figures 6, 7, and 8 show the pressure-induced intensity variation of the strongest superstructure line (511,333) for YNi_2 , GdNi_2 , and SmNi_2 , respectively. In contrast to TbNi_2 , (1) the transitions are sharper and (2) there is a complete retransformation after pressure release in all three compounds. However, the retransformation is shifted to much lower pressures in SmNi_2 and seems to be strongly smeared in YNi_2 (for GdNi_2 only the point after complete pressure release was measured). In Table I all the estimated transition pressures observed at increasing pressures are summarized.

As can be seen from Figs. 3, 6, 7, and 8, the strongest superstructure line (511,333) does not vanish completely in all the samples including TbNi_2 . This means that the pressure-induced disordering of the vacancies is not complete up to the attained pressures. However, even for YNi_2 , where the remaining intensity is largest, this would only mean that about 10% of the vacancies remain ordered. The reason for the weak remaining superstructure lines could be nonhydrostatic pressure conditions and internal strains, inhibiting a complete disordering of all vacancies in the whole sample.

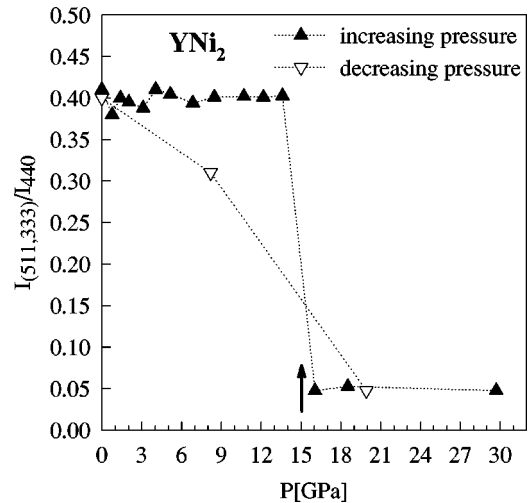


FIG. 6. Intensity ratio of the strongest superstructure line (511,333) and the (440) line [corresponding to (220) of $C15$] as a function of pressure for YNi_2 , illustrating the pressure-induced transition from the $C15$ superstructure to a structure with $C15$ symmetry. The arrow indicates the estimated transition pressure on increasing pressure (see Table I).

The variation of the volume of YNi_2 , SmNi_2 , and GdNi_2 as a function of the applied pressure has been determined from the energies of the x-ray peaks, as obtained from the energy dispersive measurements. The experimental error of the energy dispersive measurements was larger than that of the angle dispersive measurements on TbNi_2 . However, within this larger error the compressibility is the same for all four samples, i.e., the compressibility of TbNi_2 can be regarded as representative for all investigated compounds.

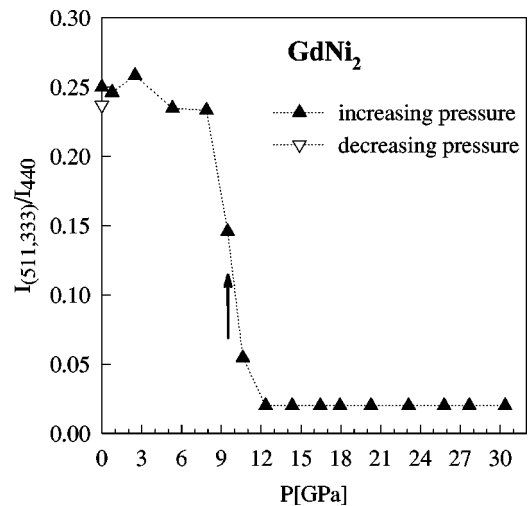


FIG. 7. Intensity ratio of the strongest superstructure line (511,333) and the (440) line [corresponding to (220) of $C15$] as a function of pressure for GdNi_2 , illustrating the pressure-induced transition from the $C15$ superstructure to a structure with $C15$ symmetry. The arrow indicates the estimated transition pressure on increasing pressure (see Table I).

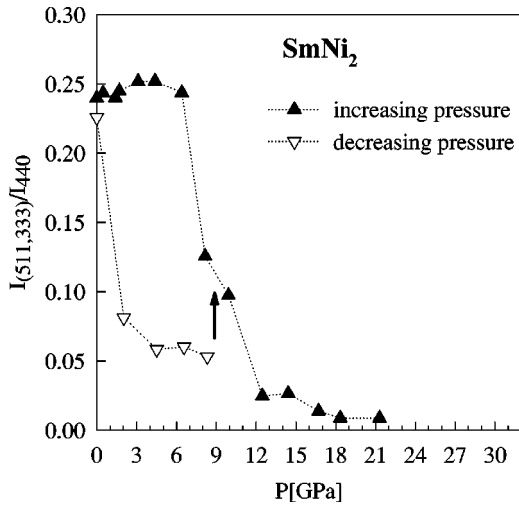


FIG. 8. Intensity ratio of the strongest superstructure line (511,333) and the (440) line [corresponding to (220) of $C15$] as a function of pressure for SmNi_2 , illustrating the pressure-induced transition from the $C15$ superstructure to a structure with $C15$ symmetry. The arrow indicates the estimated transition pressure on increasing pressure (see Table I).

V. DISCUSSION

The presented high-pressure studies on $R\text{Ni}_2$ compounds show that the earlier observed reversible structural transition from the $C15$ superstructure to a structure with $C15$ symmetry at high temperatures⁶ can also be induced by high pressure, i.e., the ordered vacancies at the R sites also become disordered (statistically distributed over all R sites) when applying high pressure. This means, that a decrease of the atomic distances has the same effect as increasing the thermal energy of the atoms. A high thermal energy is connected with a large amplitude of the lattice vibrations and can finally lead to a moving of the atoms into neighboring vacancies, to a breakdown of the correlation between the ordered vacancies, and thus to a temperature-induced disordering of the vacancies. However, the observed pressure-induced transition shows that not only a higher thermal energy of the atoms can lead to the disordering of the vacancies, but also a decrease of the distance between the vacancies and the neighboring atoms. Obviously, the movement of an R atom into a neighboring vacancy is also favored by a shorter distance to the vacancy.

The close connection between the temperature-induced and the pressure-induced order-disorder transition is confirmed by a comparison between the transition temperatures and pressures. As can be seen from Fig. 9, a high transition temperature (i.e., the necessary thermal energy leading to a

TABLE I. Transition pressures, observed at increasing pressures, for all investigated $R\text{Ni}_2$ compounds.

YNi_2	15 ± 0.5 GPa
GdNi_2	9.5 ± 1.0 GPa
SmNi_2	9.0 ± 1.5 GPa
TbNi_2	8 ± 2 GPa

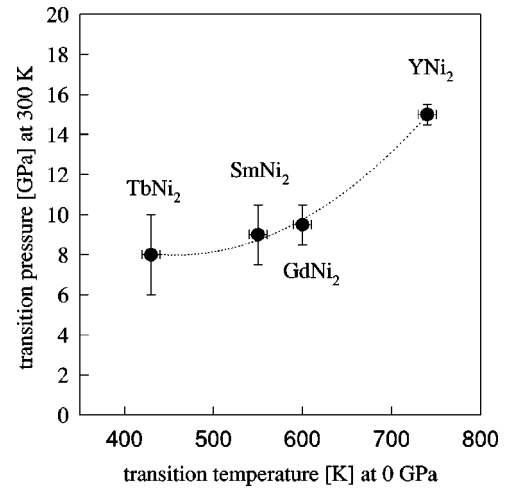


FIG. 9. Transition pressure at ambient temperature (this work, see Table I) as a function of the transition temperature at ambient pressure [taken from measurements of the electrical resistivity (Ref. 6)] for the investigated $R\text{Ni}_2$ compounds. The error bars indicate the smearing of the transitions.

disordering of the vacancies is high) is connected with a high transition pressure (i.e., a larger decrease of the atom-vacancy distance is necessary). Especially the comparison of YNi_2 with the other three compounds confirms this close connection. In YNi_2 the transition pressure as well as the transition temperature are much higher and, interestingly, the transition is also more pronounced. This can be seen from the sharper pressure-induced transition (compare Fig. 6 with Figs. 3, 7, and 8) and also from the sharper temperature-induced transition (as observed in the temperature variation of the electrical resistivity⁶). In the case of TbNi_2 the temperature-induced as well as the pressure-induced transition is least pronounced.

The main reason for the differences in the transition pressures and temperatures, as shown in Fig. 9, could be the different number of ordered vacancies. An increasing number of ordered vacancies (i.e., a smaller $4a$ occupancy) increases the correlation between them, and therefore the necessary temperature or pressure for breaking up this correlation is also higher. For the investigated YNi_2 sample the $4a$ occupancy is small (about 0.25, see above), leading to the highest transition temperature (740 K) and to the highest transition pressure (≈ 15 GPa) among all investigated $R\text{Ni}_2$ samples. The investigated TbNi_2 sample has a $4a$ occupancy of about 0.75, i.e., the number of ordered vacancies is three times smaller than in the investigated YNi_2 sample, leading to the lowest transition temperature (430 K) and pressure (≈ 8 GPa).

A second effect of a high number of ordered vacancies could be a more pronounced and sharper transition, since more vacancies are involved in the order-disorder process. The HPXRD experiments show that the sharpness of the pressure-induced transition is indeed connected with the transition pressure, i.e., the higher the transition pressure, the sharper the transition. This can be seen from the size of the error bars of the transition pressures shown in Fig. 9, or directly by a comparison of Figs. 3, 6, 7, and 8.

The compressibility (see Fig. 4) is not affected by the observed order-disorder transition, at least within the accuracy of the HPXRD experiments. High-temperature thermal expansion experiments using capacitance dilatometry⁶ showed volume effects of $\Delta V/V \approx -0.001$ at the transition, which are too small to be detectable by HPXRD experiments.

Concluding, this work showed that the earlier observed reversible temperature-induced disordering of the R vacancies in the RNi_2 Laves phase superstructures can also be induced by high pressure. Furthermore, the analysis of the correlation between the transition pressures and temperatures indicate that the driving mechanism behind the temperature-

induced and the pressure-induced transition is the same, and that the number of the vacancies might play an important role.

ACKNOWLEDGMENTS

This work has been supported by the Austrian Science Fund FWF (Project No. P-14932-PHY) and by the Austrian Academy of Sciences (Grant No. APART 10739). We also want to thank V. Paul-Boncour for fruitful discussions and R. Miletich for important advice concerning the high-pressure experiments.

¹M. Latroche, V. Paul-Boncour, A. Percheron-Guegan, and J.C. Achard, *J. Less-Common Met.* **161**, L27 (1990).

²M. Latroche, V. Paul-Boncour, and A. Percheron-Guegan, *Z. Phys. Chem. (Munich)* **179**, 261 (1993).

³A. Lindbaum, J. Hafner, E. Gratz, and S. Heathman, *J. Phys.: Condens. Matter* **10**, 2933 (1998).

⁴A. Lindbaum, J. Hafner, and E. Gratz, *J. Phys.: Condens. Matter* **11**, 1177 (1999).

⁵E. Gratz, E. Goremychkin, M. Latroche, G. Hilscher, M. Rotter, H. Müller, A. Lindbaum, H. Michor, V. Paul-Boncour, and T. Fernandez-Diaz, *J. Phys.: Condens. Matter* **11**, 7893 (1999).

⁶E. Gratz, A. Kottar, A. Lindbaum, M. Mantler, M. Latroche, V.

Paul-Boncour, M. Acet, Cl. Barner, W.B. Holzapfel, V. Pacheco, and K. Yvon, *J. Phys.: Condens. Matter* **8**, 8351 (1996).

⁷R.J. Angel, D.R. Allan, R. Miletich, and L.W. Finger, *J. Appl. Crystallogr.* **30**, 461 (1997).

⁸K. Syassen and W.B. Holzapfel, *Europhys. Conf. Abstr.* **1A**, 75 (1975).

⁹A.P. Hammersley (unpublished).

¹⁰F.D. Murnaghan, *Am. J. Math.* **49**, 235 (1937).

¹¹U. Benedict and W.B. Holzapfel, in *Handbook on the Physics and Chemistry of Rare Earths*, edited by K.A. Gschneidner *et al.*, (North-Holland, Amsterdam, 1993), Vol. 17, Chap. 113.

¹²F. Birch, *Phys. Rev.* **71**, 809 (1947).